12

Annual Report

Atomic Layer Epitaxy Group IV Materials: Surface Processes, Thin Films, Devices and Their Characterization

Office of Naval Research
Supported under Grant #N00014-91-J-1416
Report for the period 1/1/92-12/31/92

Robert F. Davis, Salah Bedair*, Nadia A. El-Masry and Jeffrey T. Glass
M. B. Ferrara, P. Goeller, S. King, J. J. Sumakeris, S. Tanaka,
L. Tye*, S. D. Wolter, P. C. Yang, and W. Zhu
c/o Materials Science and Engineering Department
and *Electrical and Computer Engineering Department
North Carolina State University
Campus Box 7907
Raleigh, NC 27695-7907

December, 1992

REPORT DOCUMENTATION PAGE

Form Approved
OMB No 0704-0188

1. AGENCY USE ONLY (Leave blank)	2. REPORT DATE	3. REPORT TYPE AND DATES COVERED
	December 1992	Annual 1/1/92–12/31/92

4. TITLE AND SUBTITLE

Atomic Layer Epitaxy Group IV Materials: Surface Processes, Thin Films, Devices and Their Characterization

5. FUNDING NUMBERS

414v001---01
RA414
068342
2B

6. AUTHOR(S)

Robert F. Davis, Salah Bedair,
Nadia El-Masry and Jeffrey T. Glass

7. PERFORMING ORGANIZATION NAME(S) AND ADDRESS(ES)

North Carolina State University
Hillsborough Street
Raleigh,NC 27695

8. PERFORMING ORGANIZATION REPORT NUMBER

N00014-91-J-1416

9. SPONSORING/MONITORING AGENCY NAME(S) AND ADDRESS(ES)

Office of the Chief of Naval Research
Electronics Division, Code 1114SS
800 North Quincy Street,
Arlington, VA 22217-5000

10. SPONSORING/MONITORING AGENCY REPORT NUMBER

11. SUPPLEMENTARY NOTES

12a. DISTRIBUTION/AVAILABILITY STATEMENT

Approved for Public Release; Distribution Unlimited

12b. DISTRIBUTION CODE

13. ABSTRACT (Maximum 200 words)

An integrated growth and surface characterization system containing a hot filament reactor, sample transfer station, ESD and XPS has been established to investigate the ALE of diamond films. Complementary experiments concerned with the nucleation of diamond on molten surfaces, e. g., Al and Ge have also been conducted. Formation of GeO_2 or an aluminum carbide and the degradation of the diamond by the molten material inhibited nucleation on the melted area. Monocrystalline thin films of β-SiC have been achieved in the temperature range of 850°–980°C by atomic layer-by-layer deposition of Si and C species via sequential exposures of Si(100) substrates to Si_2H_6 and C_2H_4. A UHV analytical system containing TPD, AES and XPS is being constructed in concert with the SiC ALE studies to determine the reaction chemistry important to this process. An eximer laser ablation system for the ALE of CeO_2 has been completed and employed to successfully deposit films of this material on Si(100).

14. SUBJECT TERMS	15. NUMBER OF PAGES
atomic layer epitaxy (ALE), diamond, silicon carbide, cerium dioxide	32
	16. PRICE CODE

17. SECURITY CLASSIFICATION OF REPORT	18. SECURITY CLASSIFICATION OF THIS PAGE	19. SECURITY CLASSIFICATION OF ABSTRACT	20. LIMITATION OF ABSTRACT
UNCLAS	UNCLAS	UNCLAS	SAR

Table of Contents

I. Introduction

Atomic layer epitaxy (ALE) is the sequential chemisorption of one or more elemental species or complexes within a time period or chemical environment in which only one monolayer of each species is chemisorbed on the surface of the growing film in each period of the sequence. The excess of a given reactant which is in the gas phase or only physisorbed is purged from the substrate surface region before this surface is exposed to a subsequent reactant. This latter reactant chemisorbs and undergoes reaction with the first reactant on the substrate surface resulting in the formation of a solid film. There are essentially two types of ALE which, for convenience, shall be called Type I and Type II.

In its early development in Finland, the Type I growth scenario frequently involved the deposition of more than one monolayer of the given species. However, at that time, ALE was considered possible only in those materials wherein the bond energies between like metal species and like nonmetal species were each less than that of the metal-nonmetal combination. Thus, even if multiple monolayers of a given element were produced, the material in excess of one monolayer could be sublimed by increasing the temperature and/or waiting for a sufficient period of time under vacuum. Under these chemical constraints, materials such as GaAs were initially thought to be improbable since the Ga-Ga bond strength exceeds that of the GaAs bond strength. However, the self-limiting layer-by-layer deposition of this material proved to be an early example of type II ALE wherein the trimethylgallium (TMG) chemisorbed to the growing surface and effectively prevented additional adsorption of the incoming metalorganic molecules. The introduction of As, however caused an exchange with the chemisorbed TMG such that a gaseous side product was removed from the growing surface. Two alternating molecular species are also frequently used such that chemisorption of each species occurs sequentially and is accompanied by extraction, abstraction and exchange reactions to produce self-limiting layer-by-layer growth of an element, solid solution or a compound.

The type II approach has been used primarily for growth of II-VI compounds [1-13]; however, recent studies have shown that it is also applicable for oxides [14-18], nitrides [19], III-V GaAs-based semiconductors [20-33] and silicon [34-36]. The advantages of ALE include monolayer thickness control, growth of abrupt interfaces, growth of uniform and graded solid solutions with controlled composition, reduction in macroscopic defects and uniform coverage over large areas. A commercial application which makes use of the last attribute is large area electroluminescent displays produced from II-VI materials. Two comprehensive reviews [37,6], one limited overview [38] and a book [39] devoted entirely to the subject of ALE have recently been published.

The materials of concern in this program include silicon carbide (SiC), diamond (C) and cerium dioxide (CeO_2). Equipment for the ALE deposition of each of these materials, as well as the experimental procedures for the conduct of these studies are in various stages of design,

development and employment. Deposition of all three materials has been achieved. The following sections introduce each topic, detail the experi-mental approaches, report the results to date and provide a discussion and a conclusion for each material. Each major section is self-contained with its own figures, tables and references.

References

1. T. Suntola and J. Antson, U.S. Patent 4,058,430 (1977).
2. M. Ahonen, M. Pessa and T. Suntola, *Thin Solid Films,* **65,** 301 (1980).
3. M. Pessa, R. Makela, and T. Suntola, *Appl. Phys. Lett.,* **38,** 131 (1981).
4. T. Yao and T. Takedâ, *Appl. Phys. Lett.,* **48,** 160 (1986).
5. T. Yao, T. Takeda, and T. Watanuki, *Appl. Phys. Lett.,* **48,** 1615 (1986).
6. T. Yao, *Jpn. J. Appl. Phys.,* **25,** L544 (1986).
7. T. Yao and T. Takeda, *J. Cryst. Growth,* **81,** 43 (1987).
8. M. Pessa, P. Huttunen and M.A. Herman, *J. Appl. Phys.,* **54,** 6047 (1983).
9. C.H.L. Goodman and M.V. Pessa, *J. Appl. Phys.,* **60,** R65 (1986).
10. M.A. Herman, M. Valli and M. Pessa, *J. Cryst. Growth,* **73,** 403 (1985).
11. V.P. Tanninen, M. Oikkonen and T. Tuomi, *Phys. Status Solidi,* **A67,** 573 (1981).
12. V.P. Tanninen, M. Oikkonen and T. Tuomi, *Thin Solid Films,* **90,** 283 (1983).
13. D. Theis, H. Oppolzer, G. Etchinghaus and S. Schild, *J. Cryst. Growth,* **63,** 47 (1983).
14. S. Lin, *J. Electrochm. Soc.,* **122,** 1405 (1975).
15. H. Antson, M. Leskela, L. Niinisto, E. Nykanen and M. Tammenmaa, Kem.-Kemi, **12,** 11 (1985).
16. R. Tornqvist, Ref. 57 in the bibliography of Chapt. 1 of Ref. 39 of this proposal.
17. M. Ylilammi, M. Sc. Thesis, *Helsinki Univ. of Technology,* Espoo (1979).
18. L. Hiltunen, M. Leskela, M. Makela, L. Niinisto, E. Nykanen and P. Soininen, *Surface Coatings and Technology,* in press.
19. I. Suni, Ref. 66 in the bibliography of Chapt. 1 of Ref. 39 in this report.
20. S.M. Bedair, M.A. Tischler, T. Katsuyama and N.A. El-Masry, *Appl. Phys. Lett.,* **47,** 51 (1985).
21. M.A. Tischler and S.M. Bedair, **48,** 1681 (1986).
22. M.A. Tischler and S.M. Bedair, *J. Cryst. Growth,* **77,** 89 (1986).
23. M.A. Tischler, N.G. Anderson and S.M. Bedair, *Appl. Phys. Lett.,* **49,** 1199 (1986).
24. M.A. Tischler, N.G. Anderson, R.M. Kolbas and S.M. Bedair, *Appl. Phys. Lett.,* **50,** 1266 (1987).
25. B.T. McDermott, N.A. El-Masry, M.A. Tischler and S.M.Bedair, *Appl. Phys. Lett.,* **51,** 1830 (1987).
26. M.A. Tischler, N.G. Anderson, R.M. Kolbas and S.M. Bedair, *SPIE Growth Comp. Semicond.,* **796,** 170 (1987).
27. S.M. Bedair in *Compound Semiconductor Growth Processing and Devices for the 1990's,* Gainesville, FL, 137 (1987).
28. J. Nishizawa, H. Abe and T. Kurabayashi, *J. Electrochem. Soc.,* **132,** 1197 (1985).
29. M. Nishizawa, T. Kurabayashi, H. Abe, and N. Sakurai, *J. Electrochm. Soc.,* **134,** 945 (1987).
30. P.D. Dapkus in Ref. 27, p. 95.
31. S.P. Denbaars, C.A. Beyler, A. Hariz and P.D. Dapkus, *Appl. Phys. Lett.,* **51,** 1530 (1987).
32. M. Razeghi, Ph. Maurel, F. Omnes and J. Nagle, *Appl. Phys. Lett.,* **51,** 2216 (1987).
33. M. Ozeki, K. Mochizuki, N. Ohtsuka and K. Kodama, *J. Vac. Sci. Technol.* **B5,** 1184 (1987).
34. Y. Suda, D. Lubben, T. Motooka and J. Greene, *J. Vac. Sci. Technol.,* **B7,** 1171 (1989).

35. J. Nishizawa, K. Aoki, S. Suzuki and K. Kikuchi, *J. Cryst. Growth,* **99,** 502 (1990).
36. T. Tanaka, T. Fukuda, Y. Nagasawa, S. Miyazaki and M. Hirose, *Appl. Phys. Lett.,* **56,** 1445 (1990).
37. T. Suntola and J. Hyvarinen, *Ann. Rev. Mater. Sci.,* **25,** 177 (1985).
38. M. Simpson and P. Smith, *Chem. Brit.,* **23,** 37 (1987).
39. T. Suntola and M. Simpson, *Atomic Layer Epitaxy,* Chapman and Hall, New York, 1990.

II. In-Vacuo Surface Analysis for the Atomic Layer Nucleation of Diamond Films

Introduction

During this report period, we have been concentrating on the establishment of an integrated hot filament CVD and UHV analytical system to allow in-vacuo surface analysis (XPS and AES) to be made on the atomic layer nucleation (ALN) of diamond films. Such a system will allow the phases (chemical bonding) formed on the substrate surface during ALN process to be characterized in a time dependent manner without ambient contaminations and thus greatly improve our understanding of the surface chemistry and growth mechanisms of the ALN process.

Results

With partial support from other ongoing programs, an integrated system coupling a hot filament CVD reactor, a sample transfer station, an ESD (electron stimulated desorption) chamber, and an XPS chamber (photoelectron spectroscopy) has been completely assembled (see the schematic diagram of the system in Figure 1). This integrated system is located in a new laboratory space recently allocated to this group on the new Centennial campus of NCSU. Vacuum leak testing and calibration of the XPS system have also been finished, while the calibration of the ESD system is still ongoing. The UHV chambers now can reach an ultrahigh vacuum of 10^{-10} torr aided by a 400l/s ion pump and a Ti sublimation pump. The XPS system is composed of a VG CLAM2 hemispherical electron energy analyzer, a VG XR3E2 x-ray source and a complete computer software for XPS and AES analysis and data processing. The CLAM2 allows higher energy resolution than most other analyzers in its price range. It has excellent signal-to-noise ratios for valence band spectral measurements and can perform angle resolved XPS readily. Preliminary testing of the XPS system on a silver sample resulted in high counts at high retarding voltage settings (see Figure 2) which suggests that the whole system is in a good operational condition. In addition, an electron gun has been purchased to allow the system to perform AES analysis in a near future.

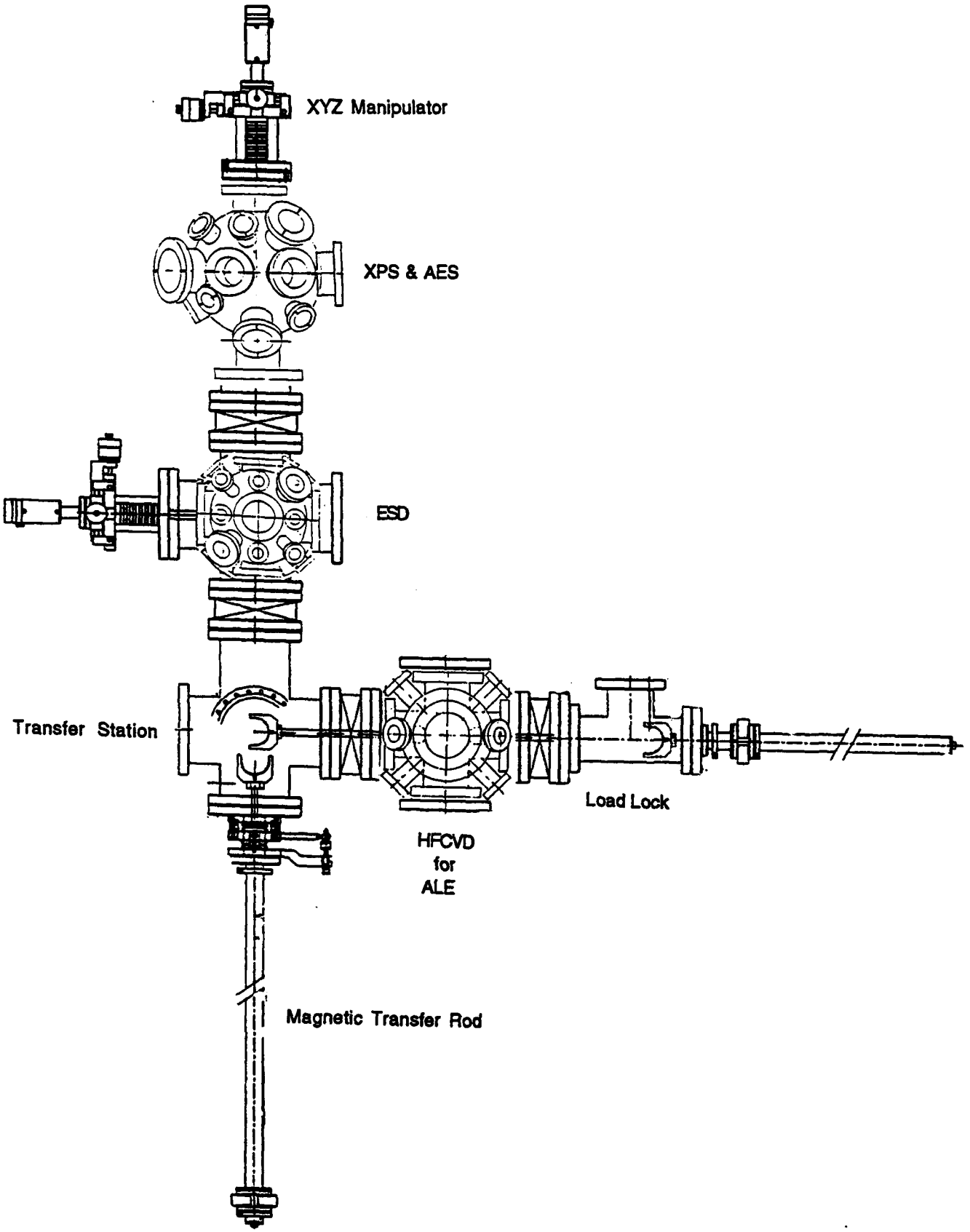

Figure 1. An integrated HFCVD and surface analysis system.

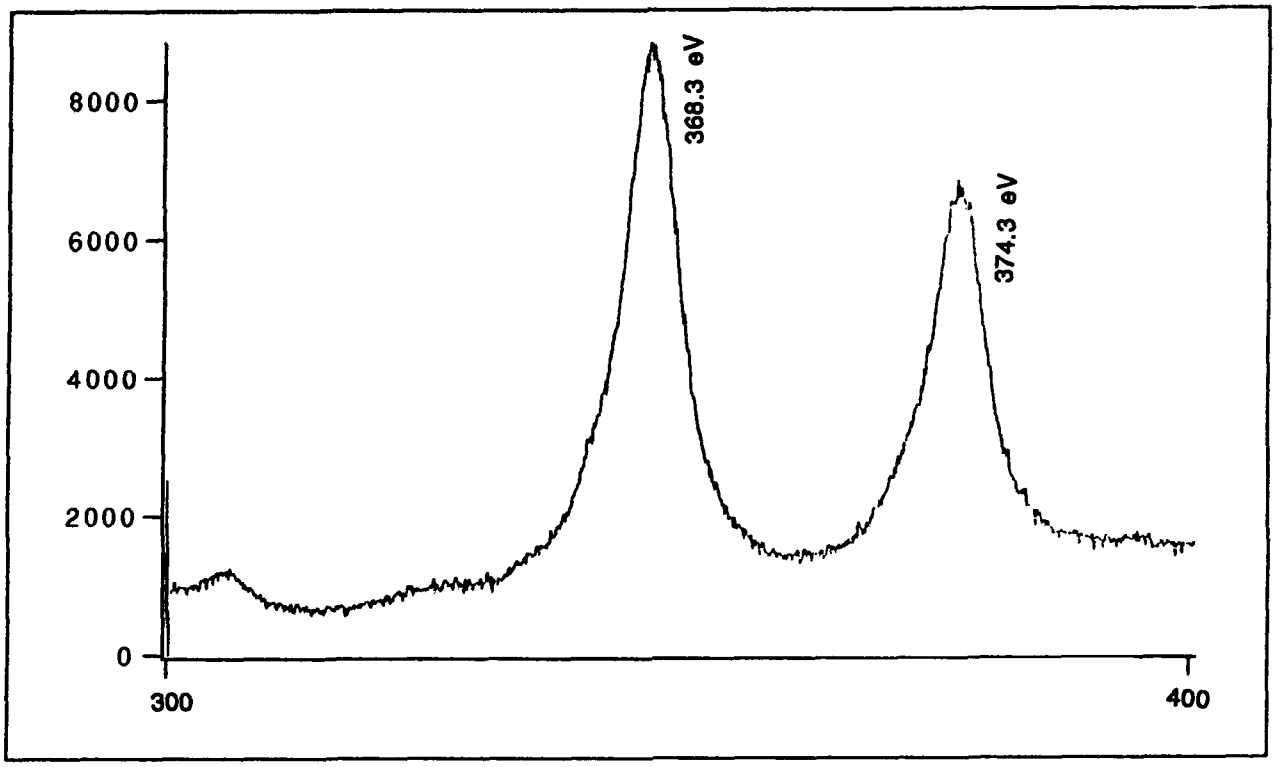

Figure 2. A calibration spectrum of Ag $3d_{5/2}$ and Ag $3d_{3/2}$.

The ESD system consists of an electron gun, an ion gun and a quadruple mass analyzer. It operates by striking an electron beam on a solid surface which results in the emission of positive and negative ions, neutrals and metastables even for primary electron beam energies as low as 10eV. By performing mass analysis and ion energy distribution or ion angular distribution, the composition, geometrical structure and bonding structure at a solid surface can be determined. Currently the whole ESD system is in a trouble-shooting stage. Although most of the components seem to be functioning, some problems have been identified in the analyzer which will need to be sent back to the manufacturer for repair.

In order to perform growth experiments which can be analyzed in-vacuo, a new hot filament CVD system has been designed and built. In addition to the capability of being able to directly coupled to the UHV analytical system, the new HFCVD chamber incorporates several new design features which alleviate many of the problems associated with diamond HFCVD reactors. The reactor is a double-walled stainless steel cross chamber with six 6" Conflat vacuum flanges and eight 2-3/4" flanges. These small flanges allow in-situ monitoring

techniques to be employed such as laser reflection interferometry and surface photo absorption (SPA) to directly control the growth process. The mounting of the filament holder on a linear translator, itself installed on an access door, allows the easy changing of the filaments with exposing the reactor to atmosphere kept to a minimum. A shutter installed between the gate valve and the chamber protects the gate valve from the attack of chemical species and particles generated in the HFCVD reactor. Another shutter mounted on a linear motion feedthrough moves between the filaments and the sample to protect the sample from tungsten contamination from the filaments during the initial carburization of the filaments.

Discussions

The research will aim to take advantage of this newly built, in-vacuo coupled growth and analytical systems to understand the fundamentals involved in the ALN process. XPS and EDS will be used in concert to evaluate the organosilicic interlayer structure and the subsequently grown films. The analytical techniques will be used by periodically stopping growth, transferring the sample to the analytical chamber, studying the sample, and then returning the sample for further growth and another cycle. The XPS will allow the determination of chemical composition of the interlayer and the nature of chemical bonding in these layers. XPS-EELS will enable the determination of the diamond content of the deposited films. ESD will allow the identification of crucial nucleation and growth species in a molecular level. It is expected that careful XPS, XPS-EELS, and ESD analyses will provide critical information about the nature of the ALN method for overcoming the high interfacial energy between diamond and non-diamond substrates for heteroepitaxy.

Conclusions

An integrated growth and surface analytical system has been established to perform in-vacuo characterization of diamond films produced via the ALN technique. The integrated system will be a powerful tool in developing clearer and coherent pictures of the surface chemistry involved in the ALN process. The acquired knowledge and information will help directly to improve design of the ALN experiments and lead to the achievement of heteroepitaxial growth of diamond films by this method

Future Work

Research in the next six months will continue the investigation of various organosilicic species (hexamethyldisilane, tetramethylsilane, and trimethylborate) in greater detail following the early work reported in the last report period. The established in-vacuo surface analytical tools are expected to play an important role in understanding the chemistry and mechanisms of the ALN process. Gas chromatography (GC) is being currently used and will be continuously used to measure and control the concentration of organosilicic species introduced into the reactor. An external substrate heater will be utilized to independently control the surface temperature during the ALN process. The ESD system will be further tested, and an electron gun and accessories will be purchased to equip the UHV chamber with AES capability. It is expected that detailed results involving these carefully designed growth and analysis experiments will be obtained and reported in the next reporting period.

III. The Effect of Molten Substrates on Diamond Deposition

A. Introduction

Diamond has an unusual combination of extreme properties that makes it an excellent material for microelectronic applications. For semiconductor applications the high thermal conductivity of diamond makes it ideal for dissipating heat from microelectronic devices. Also, the high hole mobility, the wide band gap and the high breakdown voltage of doped diamond are very desirable properties[1]. Growth of polycrystalline diamond has been achieved by many novel approaches but for use in microelectronic devices it is advantageous to deposit single crystal diamond films. This objective has been accomplished[2] as well as varying degrees of success in heteroepitaxial deposition of diamond[3,4,5,6]. However, since diamond possesses a large surface energy, three-dimensional growth is typical on non-diamond substrates. This establishes another objective, which is the nucleation and growth of two-dimensional diamond. in the present case, an atomic layer nucleation approach is of interest, which have been investigated using molten surfaces if the present study had been successful.

B. Experimental Procedure

Diamond growth was undertaken via hot filament chemical vapor deposition on both Al and Ge substrates. The substrates were polished using 600 grit SiC followed by 30μm, 6μm, and then 1μm diamond paste. The samples were further polished to remove the residual diamond seeds with .3μm followed by .05μm Al_2O_3. The substrates were then cleaned in trichloroethylene, acetone, methanol, propanol and, finally, rinsed thoroughly in de ionized(DI) water. Prior to entering into the growth chamber the substrates were seeded with 0.1μm diamond. The growth parameters for both the Al and Ge substrates were a CH_4/H_2 ratio of 1.5% performed at 100 Torr. The

temperature was increased to above 660°C for the purpose of melting the surface of the Al substrates and above 900°C to melt the Ge substrates in separate experiments. The substrates remained in a partially molten state for approximately two minutes. The substrate temperature was then reduced and the substrate was allowed to resolidify. Growth was continued at a temperature slightly below the melting point of these substrates which ranged from 5 to 30 hours. The longer growth times were utilized for the Al substrates due to lower growth temperature.

Several analytical techniques were used to investigate the Al and Ge substrates following the diamond growth. Scanning electron microscopy(SEM) was used to view the density and morphology of the diamond particles. In addition Raman spectroscopy was used to investigate the quality of the diamond on these substrates.

C. Results and Discussion

The optimum deposition temperature for low-pressure diamond growth has generally been excepted to exist between 600-1000°C. For diamond growth to be conducted on molten substrate surfaces, it was necessary for materials to be chosen with melting temperatures within this range. Al and Ge, with melting temperatures of 660 and 900°C, respectively, were found to fit this consideration.

The preliminary experiments revealed that the molten substrates would distort in the substrate holder due to the effect of surface energy. This caused the substrate's surface to transform from a very smooth surface to a rough, jagged surface. This problem was resolved by implementing a process by which only a portion of the substrate would be melted. The sample was cut into a slightly rectangular shape, and following the polishing and cleaning procedure, was placed into the chamber slightly offset from the center of the filament. The temperature was then ramped up to the melting point of the substrate. As the sample began to melt from one end of the

substrate to the other, the rate and the amount of the surface that transformed to the liquid phase could be easily controlled. The melted to unmelted region was positioned in the middle of the sample through visual inspection. Also, the unmelted to melted interface provided an accurate way to determine the exact temperature of the substrate. The deposited diamond could be investigated from the unmelted region to the melted region on both the Al and Ge substrate.

The SEM micro graphs of the Al samples revealed that the nucleation density of the resolidified molten area of the samples was significantly less than that of the unmelted portion of the substrate. This can be seen in Figure 1a and b where the diamond particles are shown on the melted and unmelted portion of the Al substrates, respectively. The quality of the diamond particles appears to be relatively high on the unmelted portion of the substrate via Raman spectroscopy.

The lack of particles on the melted portion of the substrate may be due to the degradation of the diamond seeds due to higher solubility in the molten region. The unmelted portion of the Ge substrates were either etched in the presence of CH_4 and H_2 at the elevated growth temperatures or on evaporation of the melted portion of the substrate and redeposition onto the Ge unmelted portion of the substrate. This is evident by the presence of oriented Ge hillocks that can be seen throughout the surface of the substrate in Figure 2b. No significant diamond formation was seen in this figure or on the melted portion of the substrate as seen in Figure 2a. For both Al and Ge the evaporation of these materials from the substrate may hinder the methane and hydrogen transport to the surface which may further hinder diamond formation.

D. Conclusions

Diamond deposition was attempted on both molten Al and Ge substrates. It was the intent of the authors to determine whether diamond nucleation density and

morphology could be affected by this type of surface state. No appreciable diamond was observed to have formed on either the molten Ge and Al substrates. Diamond was observed to have formed on the unmelted Al substrates but not on the Ge. The molten surface may degradate the diamonds seeds thus removing the nucleation sites in the molten region. In addition, the evaporation of the substrate material may hinder diamond growth by limiting the methane transport to the surface.

E. References

1. Gennady Sh. Gildenblat "The Electrical Properties and Device Applications of Homoepitaxial and Polycrystalline Diamond Growth" IEEE, vol. 79, no. 5, pp 647-668, (1991).

2. B.V> Spitsyn, L.L. Bouilov and B.V. Derjaguin. J. Cryst. Growth **52**, 219-226 (1981).

3. S. Koizumi, T. Inuzuka and K. Suzuki. Appl. Phys. Lett. **57**, 563-565 (1990).

4. M. Yoshikawa, H. Ishida, A. Ishitani, T. Murakami, S. Koizumi and T. Inuzuka. Appl. Phys. Lett. **57**, 428-430 (1990).

5. M. Yoshikawa, H. Ishida, A. Ishitani, S. Koizumi and T. Inuzuka. Appl. Phys. Lett. **58**, 1387 (1991).

6. D.G. Jeng, H.S. Tuan, R.F. Salat and G.J. Fricano. Appl. Phys. Lett. **67** (1990).

Figure 1a.

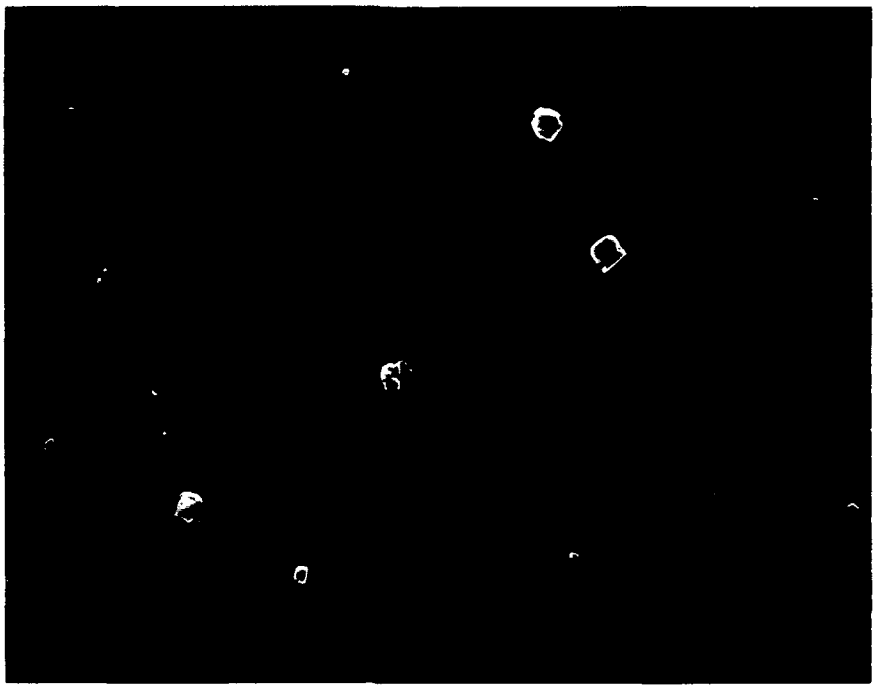

Figure 1b.

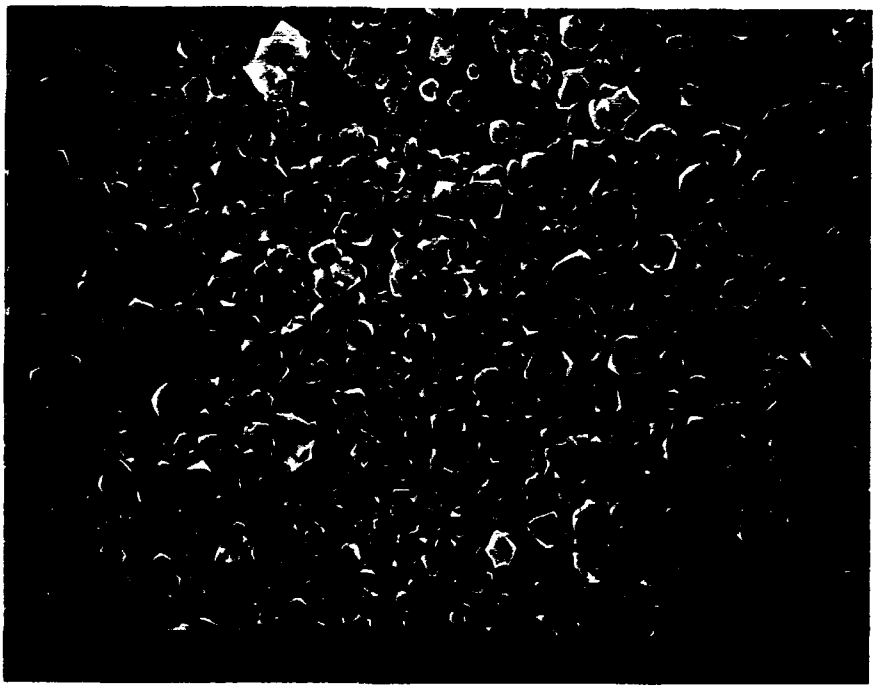

Figure 2a.

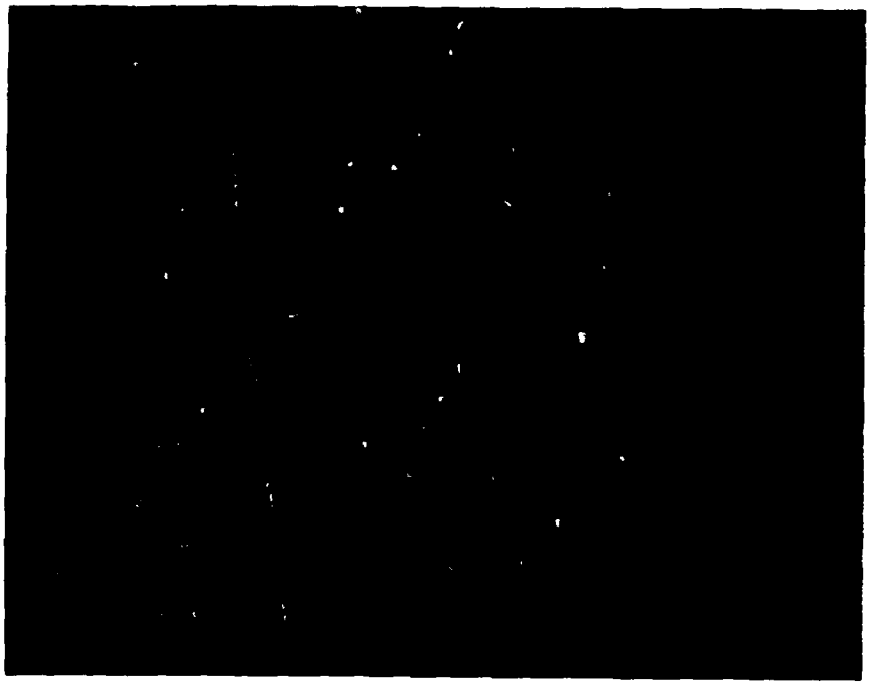

Figure 2b.

IV. Atomic Layer Epitaxy of SiC at Low Temperatures

A. Introduction

Due to it's superior thermal, mechanical and electronic properties, SiC has enormous potential for numerous applications. SiC exists in over 250 polytypes of which only one is cubic, forming in the zincblende structure and referred to as β or 3C SiC. All the remaining polytypes are hexagonal or rhombohedral [1] and are referred to collectively as α-SiC. The most common of the latter polytypes is 6H where the 6 refers to the number of Si/C bilayers of closest packed planes necessary to produce the unit cell and H refers to the hexagonal nature of the crystal. The indirect bandgaps at 300K of these two polytypes are 2.23 eV(3C) and 2.93 eV (6H), respectively [2]. Silicon carbide also possesses high values of saturated electron drift velocity (2×10^7 cm/s for 6H [3]; a slightly higher value has been predicted [4] for 3C because of reduced phonon scattering), junction breakdown electric field (5×10^6 V/cm for 6H-SiC [5]) and thermal conductivity (3.5 W/cm°C at 300 K for (6H)-SiC)[6]. These attributes taken together make SiC an attractive candidate for high-power, -temperature and -frequency devices that are resistant to radiation damage. These superior physical properties are reflected in Johnson's figure of merit which assesses the suitability of a material for discrete high-frequency and high-power devices. The normalized value for (6H)-SiC is 26.2 [7] times that of Si. Discrete devices having the potential for the aforementioned applications have been achieved and characterized in the laboratory [8,9,10]. A review of this research through 1991 has been published by Davis et. al. [11].

Epitaxial SiC films have been grown on a variety of materials, the most common substrate being that of Si(100). However, to accommodate some of the 20% and 8% mismatches in lattice parameters and coefficients of thermal expansion, respectively, between Si and SiC, the former is usually reacted with a C-containing gas to produce a thin buffer layer [12]. Subsequently, much thicker films have been grown by chemical vapor deposition (CVD) [13], plasma assisted CVD [14] and gas source molecular beam epitaxy [2].

To build high technology devices using SiC, it is desirable to grow the material at lower temperatures and in a highly conformal fashion without the necessity of growing a conversion buffer layer. Atomic layer epitaxy (ALE) offers all of these possibilities.

The objective of this research is to extend the state-of-the-art regarding SiC thin films via the employment of atomic layer epitaxy (ALE) to deposit the material on selected substrates in a layer-by-layer process. During this reporting period several key factors in the deposition of SiC were evaluated including: the role of a hot filament employed in deposition, the utility of carbonizing the Si substrate prior to ALE deposition of SiC and the parameters for monocrystalline SiC deposition were optimized. The following subsections describe the experimental procedures and discuss the results and conclusions of this research.

B. Experimental Procedure

1. ALE Reactor

The reactor used in this research has described in detail previous reports (December, 1991 and June, 1992). Within the reactor depicted in Figure 1, a rotating substrate is alternately exposed to a dose of Si_2H_6 equivalent to one monolayer of Si and an excessive exposure to C_2H_4 each revolution during deposition. The substrates rest on a receiver plate that rotates above a heater body and below a vane as shown in Figure 1. Although sample rotation is accomplished by a computer controlled stepper motor and is hence very flexible, typically a sample starts at the front zone and rotates clockwise to be exposed to Si_2H_6 on the left of the vane. As rotation continues, the sample passes through an intermediate H_2 purge zone at the back of the vane before exposure to C_2H_4 on the right side of the vane. The sample will finally return to the front zone where it will stop and reside under a hot tungsten filament that is used to enhance the surface reaction of the deposited Si and C species. The filament is approximately 0.5 cm above the substrates.

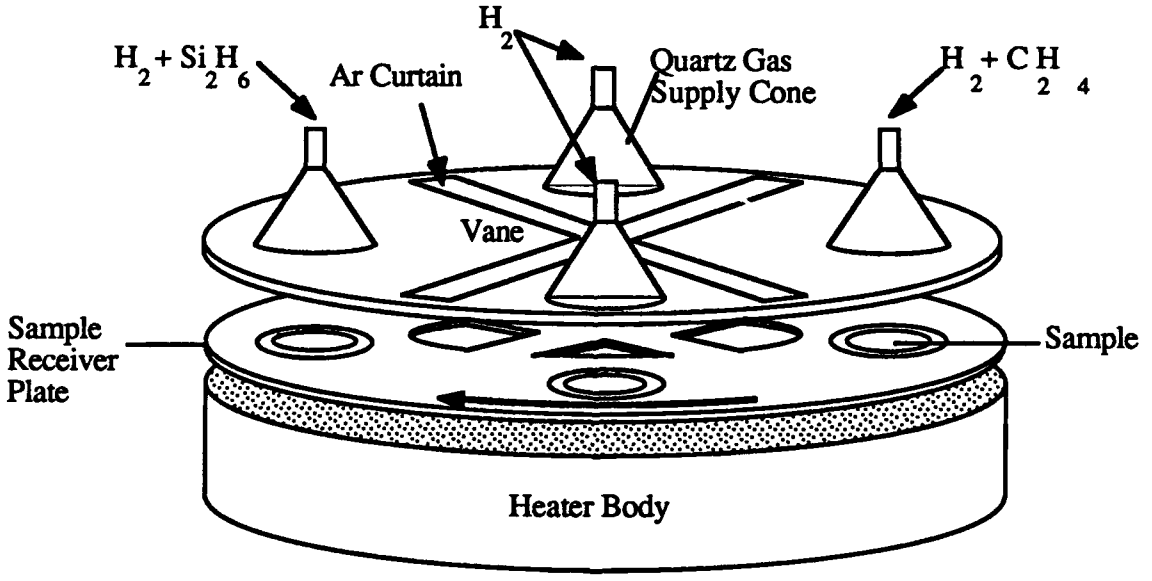

Figure 1. Internal components of ALE reactor.

Heteroepitaxial films deposited on Si(100) substrates oriented 3° off-axis toward the [011] pole have been analyzed on the basis of composition, crystallinity, growth per cycle and morphology using depth profiling Auger, RHEED, ellipsometry and TEM. Growth rate, as measured by ellipsometry and TEM, corresponded to approximately 1 monolayer per cycle. Both single crystal and highly textured polycrystalline films of β–SiC have been deposited. The potential for the growth of monocrystalline films improved significantly with extended residence time beneath the filament.

2. ALE Deposition Procedure

A typical experimental run was performed according to the following procedure. Each Si(100) substrate was RCA cleaned, immediately loaded into the system and positioned in the growth chamber within an intermediate zone. The flows of the H_2 diluent and Ar curtain gases were initiated, temperature was increased to the deposition temperature at the rate of at 10°C per minute and then samples were baked at the growth temperature for 5 minutes. The flows of Si_2H_6 and C_2H_4 were started, the filament heated and sample rotation begun. Typically each sample was rotated 360° before pausing under the filament for 30 seconds, repeating as required for desired film thickness. Once rotation was finished the sample was stopped under a H_2 purge, the Si_2H_6 and C_2H_4 flows were stopped and the filament extinguished. The sample was then allowed to cool until the sample temperature was less than 300°C when all gasses were turned off and the chamber evacuated to high vacuum. A high resolution TEM micrograph of a β-SiC film on Si (100) 3° off axis toward <011> is shown in Figure 2. The smooth interface and relatively smooth surface are evident in the micrograph as is the presence of large numbers of (111) twin defects.

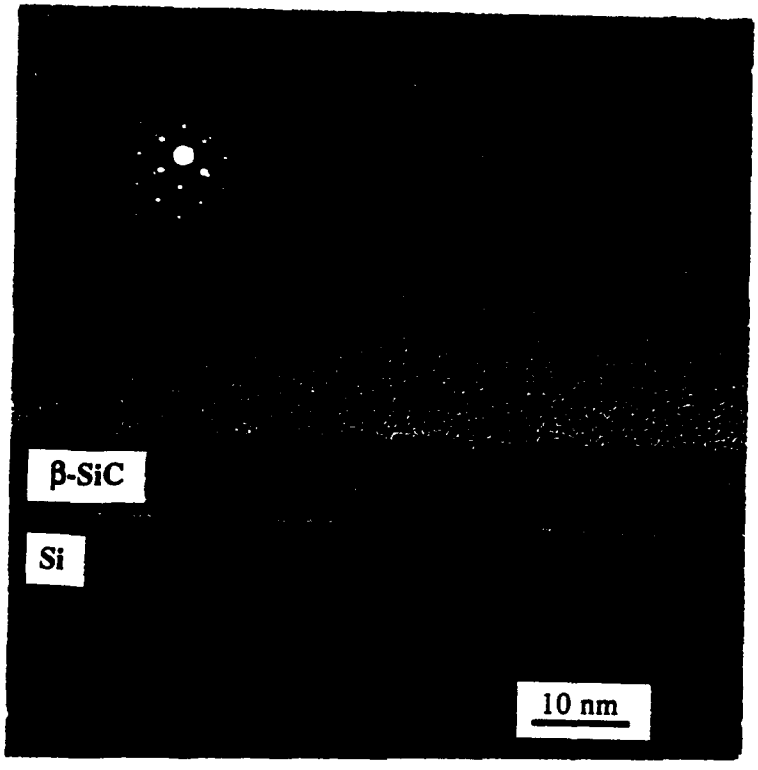

Figure 2. High resolution TEM micrograph of monocrystalline SiC film on Si (100).

Characterization of the films employed the analytical techniques of depth profiling Auger spectroscopy, RHEED, ellipsometry and TEM. Growth and characterization results and discussion of these results are presented in the following subsections for both the poly- and monocrystalline films.

C. Results

1. Role of Tungsten Filament During Deposition

Once optimal conditions for deposition of monocrystalline SiC were established, a series of six experimental runs were performed to address the effect of the heated filament during deposition. All six runs were performed under the following conditions: sample temperature = 850°C, Si_2H_6 flow rate = .8 sccm in 300 sccm of H_2, C_2H_4 flow rate = 2 sccm in 200 sccm of H_2, curtain gas flow rate = 200sccm, pause under filament for 20 seconds after each Si/ C exposure cycle. Differences between the runs and results are tabulated in Table I. The only differences in the deposition procedures were the number of cycles, whether filament was heated and what gas flowed across the filament. As can be seen from the results of runs 1-4, monocrystalline SiC can only be grown when after exposure to a Si_2H_6/C_2H_4 cycle, the sample pauses following under a hot filament over which H_2 is flowing. Further evidence that the filament plays a key role in SiC deposition is apparent in the result that for a thicker film, exposure to a hot filament during deposition results in less material deposited per cycle. It is hypothesized that any excess Si on the sample surface is removed during the samples residence below the filament. It appears that this etching is not thermal because substituting Ar gas for H_2 no longer accomplishes this etching, implying that atomic hydrogen is the etching species.

Table I. Experiments to Determine the Role of the Hot Filament in ALE of SiC

Run #	1	2	3	4	5	6
Fil. Temp	1700°C	-	1700°C	-	1700°C	-
Fil. Gas	H_2	H_2	Ar	Ar	H_2	H_2
# Cycles	50	50	50	50	600	600
Crystallinity	Single	Poly-	Poly-	Poly-	Poly-	Poly-
Thickness	-	-	-	-	1200Å	2430Å

2. Utility of Carbonizing the Si Substrate Prior to Deposition

From Table I, one can see that runs 1 and 5 were performed identically except that run 5 was run 12 times as long as run 1, resulting in a film that is polycrystalline rather than monocrystalline. While the recipe followed in run 1 can be used to grow monocrystalline films of SiC on Si as shown in Figure 2. Whenever these procedures are extended to deposit films greater than about 700Å, polycrystalline material invariably results. It appears that a morphological transition occurs during deposition of thick films. Figure 3 is a high resolution TEM micrograph of a 2100Å thick SiC film deposited on Si. RHEED reveals this to be a HIGHLY-TWINNED monocrystalline film. The film in the image appears to be monocrystalline and relatively conformal up to a thickness of ≈ 550Å after which the growth mode becomes columnar. If this experiment were continued, the resulting film would eventually become polycrystalline at the surface.

Figure 3. High Resolution TEM micrograph of SiC film on Si(100) exhibiting morphology transition.

In order to grow thicker monocrystalline films, the utility of growing conversion layers of SiC on Si prior to SiC deposition was explored with the aid of four experimental runs as depicted in Figure 4.

The results of the four carbonization experiments revealed a relationship between carbonization pre-treatment and crystallinity of the resulting film. Carbonization runs 1 and 2 gave well oriented polycrystalline films, while 3 and 4 gave Monocrystalline films. If the deposition recipe of carbonization run 3 is extended to deposit a thick films, the film becomes polycrystalline, however the recipe of carbonization run 4 has been used to grow monocrystalline SiC films on Si that are >1500Å thick.

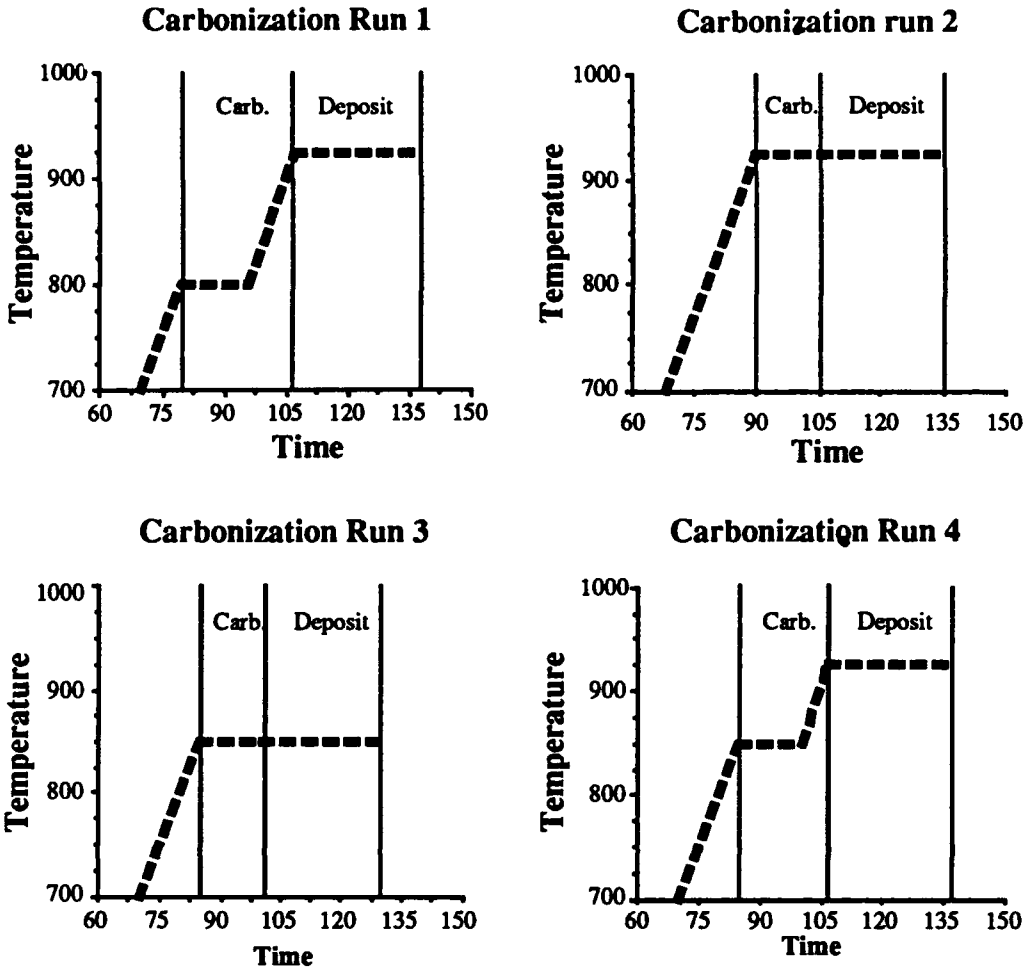

Figure 4. Carbonization experiments.

D. Discussion

Epitaxial SiC films grown on Si appear to be etched when after completing a Si/C exposure cycle they reside below a hot tungsten filament immersed in flowing H_2. This etching is expected to remove any excess Si deposited on the surface during the Si_2H_6 exposure that is not converted to SiC by the subsequent C_2H_4 exposure. This is apparently accomplished via etching by atomic hydrogen since substituting Ar for the H_2 gas does not result in detectable etching. If the excess Si atoms are not removed, they result may be the generation of a two phase film, or local disorder that may result in a polycrystalline film. To achieve the optimal SiC film morphology at any of the explored conditions requires an extended residence time below the filament.

As is the case in many CVD type operations, the deposition of SiC on Si may be best considered to occur in two separate steps: heteroepitaxial "nucleation" of the film on the original Si substrate surface and subsequent homoepitaxial deposition of SiC on the established

SiC film. Difficulties may be encountered in either phase that would compromise the quality of deposited layers.

During the formation of the initial SiC layers, it is imperative that the interface between the substrate and the film remain flat as any irregularities may encourage the nucleation of a polycrystalline film. Polycrystalline nucleation of a SiC film on a pitted Si surface is depicted in Figure 5. Also as the film first forms, there is a huge difference in lattice parameter to be accommodated, often through twinning and the formation of stacking faults. As growth continues and these defects intersect in great numbers as seen in Figure 3, regions of highly disordered material will form, encouraging columnar and eventually polycrystalline deposition. The confluence of these defects along with irregular interfaces may be responsible for much of the difficulty in depositing quality monocrystalline SiC.

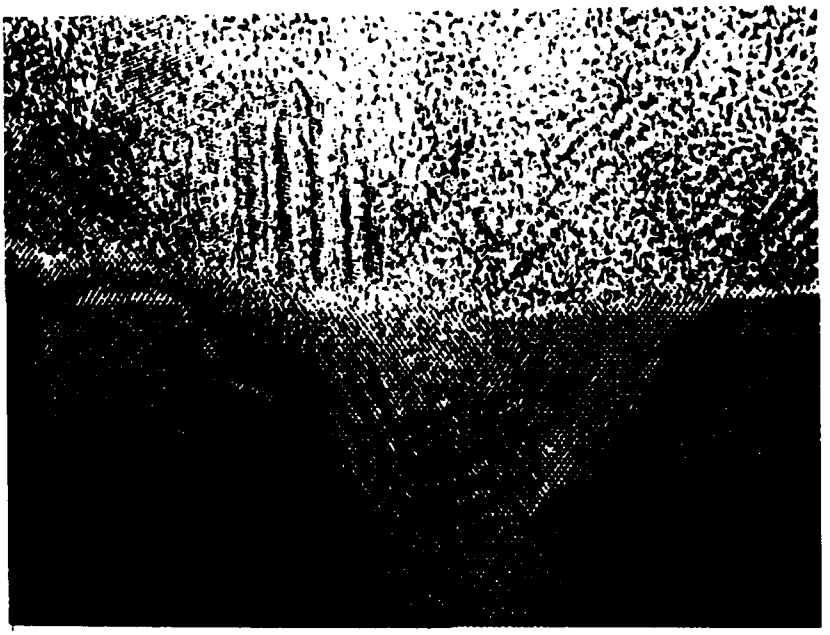

Figure 5. Voids in Si substrate used to deposit SiC.

It is known that during the carbonization of Si by hydrocarbons [14] that Si atoms from the substrate diffuse through the growing SiC layer to react with hydrocarbon molecules incident on the surface. This mass transfer may be responsible for the voids visible in the Si substrate shown in Figure 5. The major difference in the deposition recipes for the film in Figure 5 and the monocrystalline film in Figure 2 is that the latter film was deposited at a sample temperature of 850°C, almost 100°C cooler than the polycrystalline film . This behavior implies that at higher sample temperatures, the Si arriving at the sample surface from the gas phase is supplemented by Si diffusing from the substrate, probably along stacking faults and creating voids at the interface that can result in polycrystalline growth. To avoid this, the early stages of

deposition should be performed at lower temperature to limit the rate of diffusion along these defects.

As the film grows and the twin defects and stacking faults intersect, further opportunities to depart from monocrystalline growth appear. To prevent such transitions, higher sample temperatures would be preferable to "anneal out" such defects. One approach could be to deposit SiC on Si using a 2 temperature growth recipe. Starting at a lower temperature would allow "capping" the Si substrate with a thin layer (≈ 100 -to 200Å) of SiC at about 850°C, and then increase the sample temperature for subsequent deposition. This modified recipe has been employed to produce thicker SiC films on Si, but further refinement is required.

E. Conclusions

Alternating deposition of Si and C species from disilane and ethylene source gases, respectively, has been used to deposit polycrystalline and monocrystalline films of stoichiometric β-SiC on Si(100) substrates within the temperature range of 850°C to 980°C. The best monocrystalline films of SiC were grown at 850°C with extended residence time below the filament. The filament appears to remove excess Si deposited during the exposure to Si_2H_6. For thinner (< ≈500Å) SiC films on Si, a single temperature deposition routine is sufficient. Thicker monocrystalline SiC films are difficult to achieve unless a multi-temperature recipe is used, or a conversion layer is grown.

F. Future Plans

1. Address the ability to deposit SiC in trenches etched in Si wafers.
2. Attempt to dope SiC films with Al and N.
3. Construction of a cryogenic acetylene purifier is nearly complete so acetylene can be studied as a source gas for ALE growth of SiC. It is expected that the reaction of acetylene instead of ethylene with Si is more favorable for ALE growth of SiC, perhaps allowing lower temperature deposition and self-termination at the monolayer level.
4. Employ the ALE technique for construction of multilayers and solid solutions of the SiC-AlN system.
5. Attempt to deposit SiC on Si(111) by ALE. This is expected to give a more favorable growth direction for subsequent AlN deposition.

G. References

1. G.R. Fisher and P. Barnes, *Philos. Mag.* B **61**, 217 (1990).
2. T. Yoshinobu, H. Mitsui, I. Izumikawa T, Fuyuki and H. Matsunami, *Appl. Phys. Lett.* **60**, 824 (1992)

3. W. von Muench and E. Pettenpaul, *J. Appl. Phys.* **48**, 4823 (1977).
4. P. Das and D.K. Ferry, *Solid-State Electron.* **19**, 851 (1976)
5. W. von Muench and I. Pfaffender, *J. Appl. Phys.* **48**, 4831 (1977)
6. E.A. Bergemeister, W. von Muench, and E. Pettenpaul, *J. Appl. Phys.* **50**, 5790 (1979)
7. J. H. Edgar, *J. Mater. Res.* **7**, 235 (1992)
8. H. Matsunami, Optoelectronics-Devices and Technologies **2**, 29 (1987)
9. G. Kelner, M. S. Shur, S. Binari, K. J. Sleger and H. S. Kong, IEEE *IEEE Trans. Electron Devices* **36**, 1045 (1989)
10. J. W. Palmour, H. S. Kong and R. F. Davis, *Appl. Phys. Lett.* **51**, 2028 (1987)
11. R. F. Davis, G. Kelner, M. Shur, J. W. Palmour and J. A. Edmond, *Proceedings of the IEEE* **79**, 677 (1991)
12. H. Matsunami, S. Nishino and H. Ono, *IEEE Trans. Electron Devices* **28**, 1235 (1981)
13. H. S. Kong, J. T. Glass and R. F. Davis, *Appl. Phys. Lett.* **49**, 1074 (1986)
14. K. E. Haq and A. J. Learn, *J. Appl. Phys.* **40**, 431 (1969)

V. Analytical Characterization System for the Study of Atomic Layer Nucleation and Growth of Silicon Carbide

A. Introduction

Previous reports have proposed the chemistry believed necessary for the deposition of SiC by ALE. This proposed deposition mechanism was based on previous surface chemistry studies of Si_2H_6 on Si [1-4] and C_2H_4 on Si [5,6]. Unfortunately, these studies considered only the independent adsorption of each species on silicon. These studies did not look at the subsequent adsorption of a second species on top of the first adsorbed species, i.e. the adsorption of C_2H_4 on top of Si_2H_6. In order to better understand the chemistry necessary for the deposition of SiC by ALE using C_2H_4 and Si_2H_6 as precursor species, these surface chemistry studies must be expanded to include the subsequent adsorption of another species. Such studies will provide insight into the true nature of the monolayer by monolayer deposition mechanism of SiC.

The objective of this research is to extend these surface chemistry studies important to the ALE of SiC by including the subsequent adsorption of a second precursor specie. These studies will include the study of the surface adsorption and chemical reaction kinetics of Si_2H_6 and C_2H_4 on silicon, C_2H_4 on Si_2H_6 adsorbed Si, and Si_2H_6 on C_2H_4 adsorbed Si. An ultra high vacuum (UHV) system has currently been designed for these studies. The vacuum system will be composed of two chambers with several analytical techniques that include: adsorption kinetics experiments, temperature programmed desorption (TPD), X-ray photoelectron spectroscopy (XPS), Auger electron spectroscopy (AES), and X-ray photoelectron/Auger electron forward scattering experiments. The following subsections discuss and describe in more detail the UHV system and the associated analytical techniques.

B. Experimental Procedure

1. Adsorption Kinetics and Temperature Programmed Desorption (TPD)

The fist of two UHV chambers will incorporate the equipment necessary for kinetics of adsorption studies and temperature programmed desorption. A multipurpose quadropole mass spectrometer (QMS) detector design by Prof. John T. Yates, Jr., of the University of Pittsburgh (with whom we are collaborating on this research) will be used to perform both types of experiments.[7] The multipurpose QMS design consists of a QMS from Hiden Analytical Ltd. encased in a specially designed apertured chamber. The QMS chamber includes both an aperture for line of sight desorption detection as well as a fitted closure for random flux detection. This configuration allows for a variety of measurements to be made such as: absolute surface coverage determination, absolute sticking probability as a function of surface coverage, and line of sight thermal desorption.[7]

Utilizing the above mentioned apparatus, the adsorption of Si_2H_6 on C_2H_4 adsorbed on Si and vice versa will be studied. Initial studies for calibration purposes will focus on duplicating the studies of the independent adsorption of C_2H_4 and Si_2H_6 on Si. These studies will then quickly turn toward looking at the sticking probability and saturation surface coverage of Si_2H_6 on C_2H_4 adsorbed Si and vice versa. These experiments will also utilize a microcapillary array-molecular beam doser design also by Dr. John T. Yates, Jr.[8,9] This doser design will be employed due to its capability to reduce wall effects and provide a highly collimated beam of gas which represents a relatively small load to the UHV system. TPD of C_2H_4 and Si_2H_6 absorbed on one another on silicon will also be performed in order to determine the thermal stability of each species on the surface and also the species activation energy for desorption.

2. X-ray photoelectron spectroscopy (XPS) and Auger electron spectroscopy (AES)

The second UHV chamber will incorporate the equipment necessary for XPS and AES experiments. These experiments will be performed together with the adsorption kinetics/TPD experiments to enhance the information gained from both. XPS and AES will be used to provide information on the chemical composition of the silicon surfaces after exposures to various doses of C_2H_4 and Si_2H_6. The chemical shift data provided by XPS will be used to determine the type of bonding between the C_2H_4 and Si_2H_6 species and the bonding between the species and the silicon surface. AES will be primarily used to provide information on the relative concentrations of different elements at the silicon surface.

In addition to standard XPS and AES, a third analytical technique will be performed with the AES-XPS equipment. The third technique which has just recently been reviewed by Dr. William F. Egelhoff is based on some of the subtleties of the XPS and AES techniques and is referred to as X-ray photoelectron/Auger electron forward scattering.[10] In this technique, the intensity of the emitted XPS or Auger electrons are measured as function of the electrons exit angle from the surface. Electrons emitted by an atom in an XPS or Auger process are strongly forward scattered by the potential of other surrounding atoms. This forward scattering produces enhanced intensities along internuclear axes or bond directions thus giving bond angles and some structural information. This technique will therefore be used to elucidate structural information on how C_2H_4 and Si_2H_6 adsorb to the clean Si surface and the C_2H_4/Si_2H_6 saturated surfaces.

As mentioned previously, XPS, AES, and forward scattering experiments will be performed in line with the adsorption kinetics/TPD experiments. The ideal experimental sequence consists of the independent adsorption of either C_2H_4 or Si_2H_6 on Si, followed by XPS, AES, forward scattering, and TPD experiments. Ideally this whole sequence would be repeated with the adsorption of a 2nd and 3rd species.

C. Results

The results to date involve the completion of the design of both the AES-XPS system and the adsorption kinetics-TPD system. The AES-XPS system has been constructed and testing of the equipment is currently underway. All of the critical components for the adsorption kinetics-TPD system are on order and construction of this system will be underway once a "critical mass" of these components are in house. As mentioned in previous reports, both of these systems will not be a stand alone's but will be incorporated with another UHV system already in operation. This prestanding UHV system is part of the Surface Science facility here at NCSU directed by Dr. Ron Nemanich. This system currently consists of a molecular beam epitaxy (MBE) system, angle resolved ultraviolet photoelectron spectroscopy (ARUPS) system, and a plasma cleaning system. Once testing of the AES-XPS system is complete, it will incorporated with the larger surface science system. Depending on the timing of the arrival of the components for the TPD system, the TPD system may be built directly on the larger system in stead of being assembled separately.

D. Discussion

As a result of the desire to perform not only standard XPS/AES surface experiments but forward scattering experiments as well, additional design criteria were required in the design of the AES/XPS system. In order to collect the AES/XPS electron intensity as a function of exit angle from the sample surface, a nonstandard manipulator with 360 degrees of rotation about two independent axes was required. The two independent rotational axes allow the electron intensity to be measured as a function of all possible departure angles. The second design criteria crucial to the ability to perform forward scattering experiments concerns the acceptance angle of the electron energy analyzer. In order for satisfactory results to be obtained, the angular acceptance of the energy analyzer must be < 2.5 degrees which is not satisfactory for most standard AES/XPS experiments with the typical acceptance angles being approximately 7-8 degrees. Therefore the energy analyzer purchased (CLAMII from VG Microtech Ltd.) was designed to incorporate a capillary array which could be positioned to narrow the analyzers acceptance angle to approximately 1.5 degrees for forward scattering experiments and then removed for regular XPS/AES experiments.

E. Conclusions

The AES-XPS system has been constructed and testing is underway. The design of the TPD-adsorption kinetics system is complete and assembly is eminent.

F. Future Research Plans/Goals

Immediate goals include testing, and check out of the AES-XPS equipment and construction of the TPD-adsorption kinetics system.

G. References

1. J. E. Crowell, G. Lu, and B. M. H. Ning, Mat. Res. Soc. Symp. Proc., **253** (1991).
2. K. J. Uram and U. Jansson, J. Vac. Sci. Technol. **B7**, 1176 (1989).
3. S. K. Kulkarni, S. M. Gates, C. M. Greenlief, and H. H. Sawin, Surface Science **239**, 26 (1990).
4. Y. Suda, D. Lubben, T. Motooka, and J. E. Greene, J. Vac. Sci. Technol. **A8**, 61 (1990).
5. C. C. Cheng, R. M. Wallace, P. A. Taylor, W.J. Choyke, and J.T. Yates, J. Appl. Phys. **67**, 3693 (1990).
6. C. C. Cheng, W.J. Choyke, and J. T. Yates, Surface Science **231**, 289 (1990).
7. V. S. Smentkowski and J. T. Yates, Jr., J. Vac. Sci. Technol. **A7**, 3325 (1989).
8. A. Winkler and J. T. Yates, Jr., J. Vac. Sci. Technol. **A6**, 2929 (1988).
9. M. J. Bozack, L. Muehlhoff, J. N. Russel, Jr., W. J. Choyke, and J. T. Yates, Jr., J. Vac. Sci. Technol. **A5**, 1 (1987).
10. W. F. Egelhoff, Jr., Critical Reviews in Solid State and Materials Sciences **16**, 213 (1990).

VI. Epitaxial Growth of CeO_2 on Si

A. Introduction

The growth of epitaxial ceramic thin films on silicon is of interest for applications to high quality silicon-on-insulator (SOI) layers and stable capacitor devices. CeO_2 is an excellent candidate for such an insulator, having the cubic fluorite structure, with the lattice misfit factor $\Delta a/a$ for CeO_2 to Si being 0.35%.[1] Also, CeO_2 has a dielectric constant of ~26, which could potentially allow it to be used in stable capacitor devices of small dimensions.[1]

It has been shown that crystalline layers of CeO_2 may be grown on a Si substrate by means of laser ablation.[2,3] This process can be accomplished by irradiating a solid CeO_2 target with a high energy pulse from an excimer laser under ultra-high vacuum (UHV). This produces a "plume" of CeO_2 molecules free to move in UHV and form epitaxial layers on the Si substrate. By controlling the energy, frequency and length of the laser pulses, one hopes to achieve layer by layer growth of the oxide.

B. Experimental Procedure

System Description. The deposition system for CeO_2 consists of several parts. The vacuum system has been assembled and tested. Background pressure in the growth chamber is 1×10^{-9} torr. Lower pressures may be achieved through baking out the chamber. Incorporated into the vacuum system are *in situ* characterization equipment. A quadrupole mass spectrometer (QMS), a reflection high-energy electron diffraction (RHEED) system, and ion pressure gauges have been installed.

The laser used in deposition has been mounted on an optical table and was tested prior to use in an experiment. The excimer gas mixture used is ArF with a He buffer. This yields ultra-violet light (193nm) with energy densities as high as 180 mJ/cm^2. The unfocused beam size is 2.2cm by 1.0cm. The pulse to pulse stability was measured and calculated to be +/- 4% over ≈20K pulses.

An optical system has been devised to deliver the laser beam into the vacuum chamber and focus it to a spot approximately 2mm by 1mm. This delivery system consists of three mirrors, a lens and their respective mounts. Due to the geometry of the system, a custom beam steering device is used to direct the laser down into the chamber. Because the 193 nm line is out of the visible spectrum, a 4 mW HeNe laser is used to help aim the excimer into the growth chamber. Figure 1 shows the components of the CeO_2 laser ablation system.

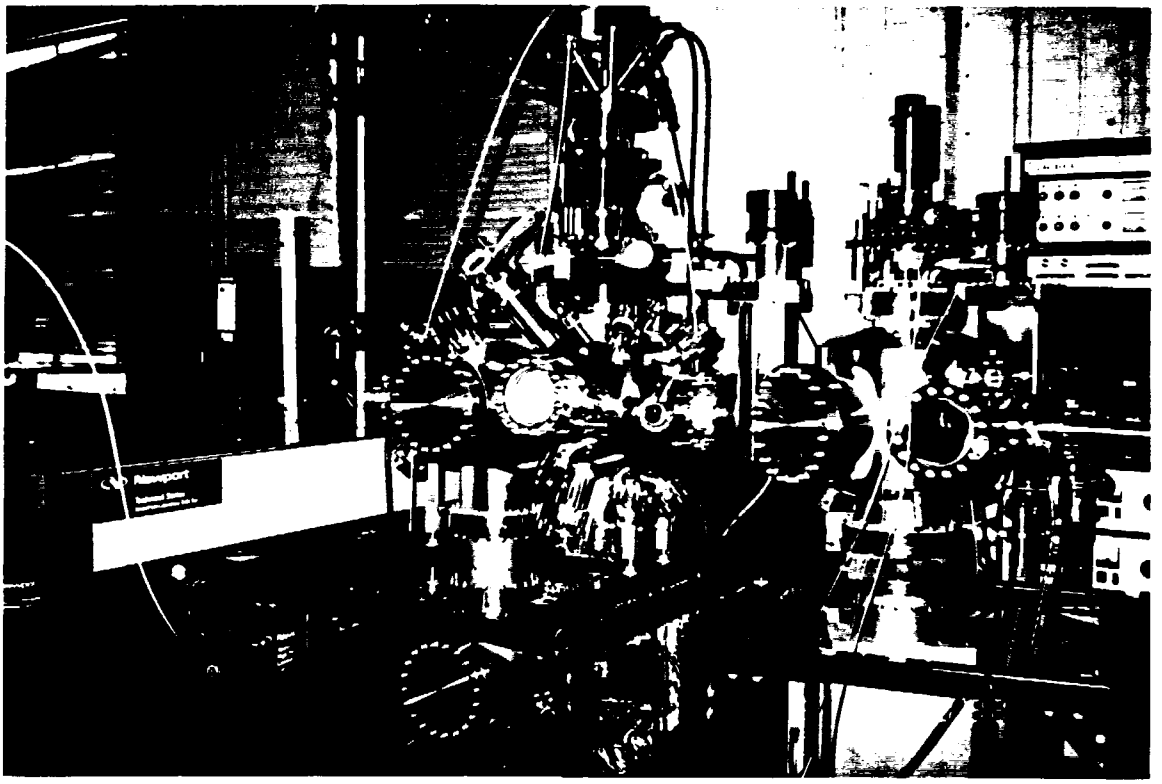

Figure 1. CeO_2 laser ablation system.

Thin film deposition. Our preliminary effort is to deposit CeO_2 on Si (100) substrate. In initial experiments, a charging voltage of 26kV was used for the excimer laser. This produced a beam with an energy density of ≈ 160 mJ/cm^2 +/- 4%. This beam was then focused to a small spot on a CeO_2 target with a theoretical energy density of 16 J/cm^2. However, due to energy losses from absorption by water vapor in air and the inefficiency of the optic delivery system, the estimated energy density arriving at the CeO_2 target was 1 to 2 J/cm^2. This value is compatible with energy densities used by other researchers. [2] Initially pulse repetition rates of 2 Hz and pulse widths of 10 ns were employed. The limit vacuum before growth was 1×10^{-9}torr. Pressure rose to 2×10^{-7}torr during ablation. The substrate temperature was maintained at ≈650 °C during growth by means of a quartz lamp heater. For initial experiments, a total of 10000 laser pulses were used per run.

Characterization of thin films. A quadrupole mass spectrometer (QMS) was used to detect residual gases and observe the oxidation state of the ablated CeO_{2-x}. During the runs, peaks at 140 amu, corresponding to Ce, and at 172 amu, corresponding to CeO_2, were observed. *Ex situ* characterization methods will include transmission electron microscopy (TEM), profilometry to determine thickness of films, and x-ray diffraction.

C. Results

Initial experiments yielded highly satisfactory results. Upon removal from the vacuum system, a CeO_2 film was immediately visible to the naked eye. The film varied in thickness and showed multi-colored fringes. A profilometer measurement indicated that the film was 0.45 μm at the thickest point. Data from this measurement is shown in Figure 2. This indicates a growth rate was ≈ .4 Å per pulse, which is less than the 1 monolayer per cycle rate desired. Thus the growth procedure needs to be optimized. Double crystal x-ray diffraction was performed, and splitting was observed around the Si(113) peak. X-ray diffraction using a Weissenberg diffractometer was also performed. Results from these measurements indicate that the CeO_2 film deposited was cubic polycrystalline with a lattice parameter of ≈5.35Å. Since the lattice parameter of CeO_2 is 5.41Å and the lattice parameter of CeO is 5.09Å, the film deposited can be assumed to be slightly oxygen deficient.

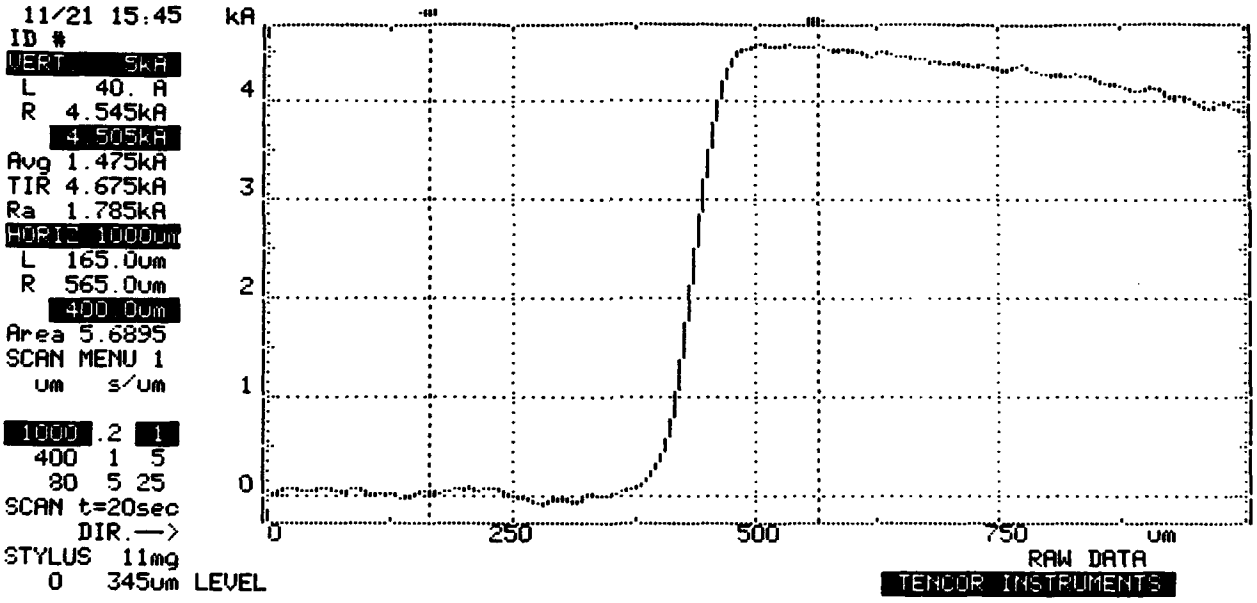

Figure 2. Profilometer data for CeO_2 film thickness

D. Discussion

Achieving growth of CeO_2 on Si on the first try is extremely satisfying, however, there is much work to be done. Some components of the system have yet to be brought on-line. The epitaxy process must be optimized to achieve uniform, layer-by-layer growth. Refinements to the system will include rotating the substrate during growth to help obtain uniform coverage of the oxide. The CeO_2 target holder will also be modified to be capable of continuous rotation during ablation. This will help maintain a constant plume shape by spreading the wear on the

target over more area. The distance from the target to the substrate must be optimized in conjunction with laser energy and pulse duration in order to achieve atomic layer epitaxy. The reflection high-energy electron diffraction (RHEED) system, while already installed on the vacuum chamber, has yet to be incorporated into the growth procedure. This *in situ* characterization tool will eventually allow atomic layer control of the growth. Also, the excimer laser performance can be improved by better alignment of the internal mirrors in the laser cavity and further alignment of the external optical delivery system.

E. Conclusions

The system for epitaxial growth of cerium oxide is currently functioning and providing results. The procedure can be refined to achieve atomic layer control of CeO_2 epitaxy on Si.

F. Future Research Plans

The perfection of the CeO_2 growth process by means of refinements to the epitaxy process as discussed above is the immediate order of business.

G. References

1. T. Inoue, Y. Yamamoto, S. Koyama, S. Suzuki, and Y. Ueda, Appl. Phys, Lett., **56**, 1332 (1990).
2. M. Yoshimoto, H. Nagata, T. Tsukshara, and H. Koinuma, Jpn. J. Appl. Phys., **29**, L1199 (1990).
3. H. Koinuma, H. Nagata, T. Tsukshara, S. Gonda, and M. Yoshimoto, Extended Abstracts of the 22nd Conference on Solid State Devices and Materials, Sendai, Japan, 1990 p. 933.
4. O. T. Sørensen, J. Solid State Chem. **18**, 217 (1976).
5. C. N. Afonso, R. Serna, F. Catalina, and D. Bermejo, Appl. Surf. Sci. **46**, 249 (1990).
6. P. Tiwari, "In-Situ Laser Processing of High Tc Superconductor and Semiconductor Heterostructures" Doctorate Thesis, Dept. of Materials Science and Engineering, NCSU, 1991.

VII. Distribution List

Mr. Max Yoder Office of Naval Research Electronics Division, Code: 1114SS 800 N. Quincy Street Arlington, VA 22217-5000	3
Administrative Contracting Officer Office Of Naval Research Resident Representative The Ohio State University Research Center 1960 Kenny Road Columbus, OH 43210-1063	1
Director, Naval Research Laboratory ATTN: Code 2627 Washington, DC 20375	1
Defense Technical Information Center Bldg. 5, Cameron Station Alexandria, VA 22314	12